Journal of Computer-Aided Molecular Design, 1 (1987) 219–241
ESCOM

J-CAMD 016

Molecular dynamics simulations of cyclosporin A: The crystal structure and dynamic modelling of a structure in apolar solution based on NMR data

J. Lautz[a,*], H. Kessler[a], R. Kaptein[b] and W.F. van Gunsteren[b]

[a]*Institut für Organische Chemie der J.-W.-Goethe-Universitat Frankfurt, Niederurseler Hang, D-6000 Frankfurt 50, F.R.G.*
[b]*Department of Physical Chemistry, University of Groningen, Nijenborgh 16, 9747 AG Groningen, The Netherlands*

Received 6 August 1987
Accepted 1 September 1987

Key words: Cyclosporin A; Restrained molecular dynamics simulation; NOE

SUMMARY

The conformation of the immunosuppressive drug cyclosporin A (CPA), both in apolar solution and in crystalline state, has been studied by computer simulation techniques. Three molecular dynamics (MD) simulations have been performed: one modelling the crystal structure and two modelling the structure in apolar solution, using a restrained MD approach in which data from nuclear magnetic resonance (NMR) and infrared (IR) spectroscopy are taken into account. The simulation of the crystalline state (MDC) concerns a system of 4 unit cells containing 16 cyclosporin A molecules and 22 water molecules, which is simulated using crystalline periodic boundary conditions. The simulations modelling the apolar solvent conformation (MDS) concern one isolated cyclosporin A molecule. In these simulations an extra term in the interatomic potential function is used, which forces the molecule to satisfy a set of 57 atom-atom distance constraints originating from nuclear Overhauser effects (NOEs) obtained from NMR spectroscopy and one distance constraint deduced from IR spectroscopy.

From a comparison of the results of the crystal simulation to those of the X-ray experiment in terms of structure, atomic fluctuations, hydrogen bond pattern, etc., it is concluded that the force field that is used yields an adequate representation of crystalline cyclosporin A. Secondly, it is shown that the dynamic modelling technique that is used to obtain a structure in a polar solution from NMR distance information works well. Starting from initial conformations which have a root mean square difference of 0.14 nm both distance restrained MD simulations converge to the same final solution structure. A comparison of the crystal structure of cyclosporin A and the one in apolar solution shows that there are significant differences. The overall difference in atomic positions is 0.09 nm for the C_α atoms and 0.17 nm for all atoms. In apolar solution, the molecule is slightly more bent and the side chains of 1 MeBmt and 10 MeLeu adopt a different conformation.

*To whom correspondence should be addressed.

INTRODUCTION

For the understanding of drug-receptor interactions, a detailed knowledge of both the conformation of the drug and of the receptor is required. However, weak intermolecular interactions due to solvent effects or receptor binding may change the conformation of the drug, its receptor or both [1,2]. One source of knowledge with respect to the conformations of a drug molecule that are accessible to it under specific environmental conditions is the crystal structure obtained from X-ray diffraction. However, a crystalline conformation may differ from the conformation in solution due to the difference between solvent and crystal packing effects [3,4].

In the last decade, it has become possible to use a variety of two-dimensional nuclear magnetic resonance (NMR) experiments [5], which yield structural information on a drug molecule in solution [6–9]. In general, the information from NOEs is derived in the form of a set of upper and lower bounds to distances between pairs of atoms in the molecule. Using graphical display techniques it is then possible to build a solution structure that satisfies all NMR data. These static model building procedures become cumbersome when large molecules with many distance constraints are at hand. In that case dynamic modelling procedures [10–12], which make use of molecular dynamics (MD) computer simulation techniques, will be efficient in deriving a solution structure.

Cyclosporin A (CPA) is a cyclic undecapeptide (see Fig. 1) with potent immunosuppressive properties [13–17]. An X-ray structure is known [18] and, in addition, a structure in apolar solution has been derived on the basis of NMR data [19] by applying static modelling techniques [18].

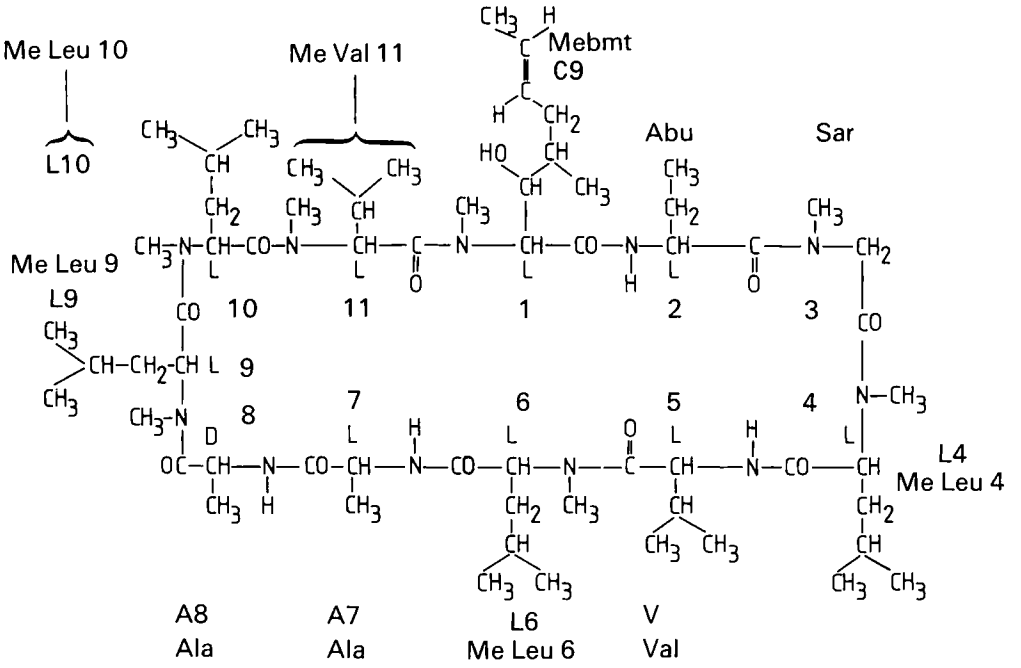

Fig. 1a. Primary structure of cyclosporin A.

Here, we will derive a better refined structure for cyclosporin A, in apolar solution by applying dynamic modelling techniques, using restrained MD simulations [10–12, 20]. Because of the relatively large set of atom-atom distance constraints (58 distances) for this cyclic peptide (49 dihedral angle degrees of freedom) in apolar solution, it forms an ideal case for testing the power of restrained MD refinement techniques.

The crystal structure of cyclosporin A [18] is considered to consist of two structural regions. (i) A β fragment consisting of residues 11 to 7, which form an anti-parallel β-pleated sheet with a type-II' β-turn [21] at residues 3 and 4. Three hydrogen bonds bridge the two short β-strands (Fig. 1b). (ii) The second fragment, a loop, is formed by the residues 7 to 11, and contains the fourth intramolecular hydrogen bond N8-H...C6, a γ'-turn of the type C_7 [22]. In position 8 there is a D-amino acid (D-Ala-8). Between the residues 9 and 10 there is a *cis* amide bond. Another remarkable feature is the position of the N-methyl group of 11-MeLeu, which points towards the center of the loop: it seems to stabilize the loop fragment by close van der Waals interactions. (iii) In addition, there is a fifth intermolecular hydrogen bond between the OH-group of the MeBmt-side chain and the carbonyl oxygen of residue 9 of a neighbouring cyclosporin A molecule in the unit cell.

In a previous study of the structure in apolar solution [18,19], a static model was built using the information from NMR and starting from the X-ray structure. The proposed apolar solution structure of the backbone contains, in general, similar structural elements as the crystal structure, except for the intermolecular hydrogen bond. However, a hydrogen bond N8-H...08 within residue 8 (D-Ala 8) was proposed on the basis of NMR experiments. In addition, the MeBmt side chain which is folded over the backbone in the crystal structure exhibits an extended conformation in apolar solution with increasing mobility along the chain beginning from the C_γ-atom. The most stable conformation of the 10-MeLeu also differs in apolar solution from that in the crystal.

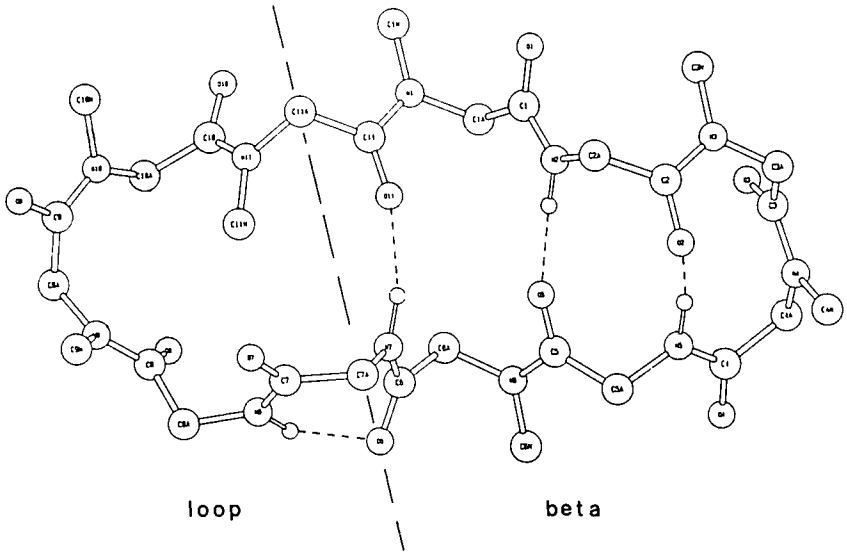

Fig. 1b. Backbone conformation of crystalline cyclosporin A with indication of the loop and β-sheet fragment.

In this paper the following three points will be addressed: (i) In order to test the molecular model and force field a system consisting of 4 cyclosporin A crystalline unit cells was simulated, using MD and a detailed comparison of simulated and measured properties of crystalline cyclosporin A was made. (ii) A refined solution structure of cyclosporin A in apolar solution based on NMR data is derived by dynamic modelling using restrained MD simulations. This structure is compared to the previously found apolar solution structure [18,19] and to the crystal structure [18]. (iii) By comparing the MD simulation of cyclosporin A in apolar solution with the MD simulation of crystalline cyclosporin A, it is possible to derive not only structural but also dynamical differences between cyclosporin A in apolar solution and in the crystalline state.

MATERIALS AND METHODS

Molecular model and force field

The programs used for performing the molecular dynamics simulations and the analysis of cyclosporin A were taken from the GROMOS (Groningen Molecular Simulation) program library.

The potential energy function describing the interaction between the N_{at} atoms is the following

$$V(r) = V(r_1, r_2, r_3 \ldots r_{N_{at}})$$

$$\sum_{l=1}^{N_b} \frac{1}{2} K_{b_l}[b_l - b_{0_l}]^2 + \sum_{l=1}^{N_\theta} \frac{1}{2} K_{\theta_l}[\theta^l - \theta^{0_l}]^2 + \sum_{l=1}^{N_\xi} \frac{1}{2} K_{\xi_l}[\xi_l - \xi_{0_l}]^2$$

$$+ \sum_{l=1}^{N_\varphi} K_{\varphi_l}[1 + \cos(n_l\varphi_l - \delta_l)] + \sum_{i<j}^{N_{at}} [C_{12}(i,j)/r_{ij}^{12} - C_6(i,j)/r_{ij}^6 + q_i q_j/(4\pi\varepsilon_0\varepsilon_r r_{ij})]$$

$$+ \sum_{l=1}^{N_{dc}} V_{dc}(r_l, r_l^0, r_l^1) \qquad (1)$$

Except for the last term, it is of the usual type applied to proteins, and is composed of terms representing covalent bond stretching, bond angle bending, harmonic (out-of-plane, out-of-tetrahedral configuration) dihedral bending, sinusoidal dihedral torsion, van der Waals and electrostatic (Coulomb) interactions. The last term of Eq. 1 was added in order to let the molecule satisfy a set of NOE distance constraints which was used for the dynamic modelling of the solution structure in apolar solution but omitted in the simulation of the crystal.

The cartesian position vectors for the N_{at} atoms are denoted by r_1, r_2, ... $r_{N_{at}}$. Hydrogen atoms attached to carbon atoms are incorporated into the latter as united atoms, whereas all hydrogen atoms, which may form hydrogen bonds, are treated explicitly. However, with respect to the last term in Eq. 1, the distance constraint term, all hydrogen or pseudo atoms, to which the NOE constraints refer, are explicitly taken into account [20].

In the first term of Eq. 1, the summation runs over all bond lengths in the molecule. However, when all bond lengths are rigidly constrained to their ideal values b_{0_l} in the simulations (see below), this term is omitted from the potential energy function. In the second term of Eq. 1, the sum-

mation runs over all N_θ bond angles l occurring in the peptide. The current value of angle l is denoted by θ_l and the force constants K_{θ_l} and minimum energy (or ideal) bond angles θ_{0_l} are parameters of the potential energy function. The dihedral angles are divided into two types: dihedrals ξ that keep certain atoms near planar or tetrahedral configurations, obeying a harmonic potential, and dihedrals that may perform complete (360°) rotations, obeying a sinusoidal potential. Lists of the parameters of the first four terms of Eq. 1 will be given elsewhere. For the relative dielectric permittivity in Eq. 1, we used a value of $\varepsilon_r = 1$. The values of the nonbonded interaction parameters $C_{12}(i,j)$ and $C_6(i,j)$, and the partial atomic charges q_l have been published [23].

However, when these van der Waals parameters were used for united atoms that are separated by three covalent bonds (third neighbours), they induce a too large repulsion in gauche conformations. In order to avoid this effect, smaller van der Waals parameters were used for united atoms separated by three covalent bonds [24]. The summation of the nonbonded interaction term runs over all atom pairs separated by more than two covalent bonds. A cut-off radius of $R_{cut} = 0.8$ nm is applied, beyond which no interactions are included. This value must be chosen smaller than half the value of the smallest edge of the periodic box used for the simulation of the crystal ($2a = 2b = 2.7674$ nm). The cut-off radius R_{cut} is applied to the centres of geometry of neutral atom groups in the peptide and to the oxygen atoms of water molecules, in order to avoid the breaking of the charge neutrality of a group or water molecule in case an atom-atom cut-off is applied.

All bond lengths of the molecules are kept rigid by applying the SHAKE-method with a relative tolerance of 10^{-4} to which the bond-length constraints are satisfied geometrically [25,26]. Water molecules are modeled by a simple rigid three point charge model (SPC) [27].

A special feature of this force field is the last term in the potential energy function Eq. 1. This term enables one to apply constraints derived by NMR measurements of NOE spectra, in order to model the solution structure of a molecule. The potential chosen was of a simple form and used only to model attractive constraints. An attractive constraint l with length r_l^0 between atom n and m is represented by [20]:

$$\begin{aligned} V_{dc}(r_{nm}, r_l^0, r_l^1) &= 0 && \text{if } 0 \leqslant r_{nm} \leqslant r_l^0 \\ &= \frac{1}{2} K_{dc}(r_{nm} - r_l^0)^2 && \text{if } r_l^0 \leqslant r_{nm} \leqslant r_l^1 \\ &= \frac{1}{2} K_{dc}(2r_{nm} - r_l^0 - r_l^1)(r_l^1 - r_l^0) && \text{if } r_{nm} \geqslant r_l^1 \end{aligned} \tag{2}$$

In this work, we chose $r_l^1 = \infty$ for all distance constraints, which results in a harmonic restraint potential. If the distance r_{nm} satisfies a given distance constraint r_l^0, the extra term will be equal to zero, otherwise if the distance is too large it will try to reduce it.

We note that the indices n and m in Eq. 2 may not only refer to real atoms, which are explicitly simulated, but also to virtual or pseudo atoms [28]. Since in the molecular model that is used, hydrogen atoms attached to carbon atoms are incorporated into the latter, i.e. are not explicitly treated, these hydrogens are called virtual atoms. The concept of a pseudo atom is used when the assignment of a distance constraint to an atom pair is not stereospecific, e.g. C_β protons or methyl groups of Leu and Val, or when the atom pair cannot be identified because of dynamic effects,

such as rotation of methyl groups and flipping of aromatic rings. In these cases the centre of geometry of the C_β protons or the two methyl groups or of the protons over which a dynamical average has to be taken, is referred to as a pseudo atom. In the last term in Eq. 2 the indices n and m may refer to these virtual or pseudo atoms, which are massless points, whose positions are rigorously related to the positions of the real atoms (with mass not equal to zero) in the molecule. When using pseudo or virtual atoms, two additional steps are to be added to the MD algorithm, as it is explained in Ref. 20.

Molecular dynamics algorithm

MD computes a trajectory of a system of N_{at} atoms by solving Newton's equations of motion for each atom i

$$\frac{d^2\boldsymbol{r}_i(t)}{dt^2} = a_i(t) = \frac{F_i(t)}{m_i} \tag{3}$$

with

$$F_i(t) = -\frac{\delta}{\delta \boldsymbol{r}_i} V(\boldsymbol{r}_1(t), \boldsymbol{r}_2(t), \ldots \boldsymbol{r}_{N_{at}}(t)) \tag{4}$$

The vectors $\boldsymbol{r}_1, \ldots \boldsymbol{r}_{N_{at}}$ represent the cartesian coordinates of each atom i with a mass m_i. The potential $V(\boldsymbol{r}_1(t), \ldots \boldsymbol{r}_{N_{at}}(t))$ used is that of Eq. 1. Performing a MD run, the 3 N_{at} coupled differential equations (3) are integrated by using small time steps. Δt, yielding trajectories for all N_{at} atoms. For the integration of Eq. 3, the leap-frog algorithm is used [29]. The total energy of the system $E_{tot}(t)$ is the sum of the potential energy $V(\boldsymbol{r}_1(t), \boldsymbol{r}_2(t), \ldots \boldsymbol{r}_{N_{at}}(t))$ and the kinetic energy:

$$E_{kin}(t) = \sum_{i=1}^{N_{at}} \frac{1}{2} m_i v_i^2(t) \tag{5}$$

Using Eq. 5, one can easily obtain the temperature T(t) of the system:

$$T(t) = E_{kin}(t)/(\frac{3}{2} N_{at} k) \tag{6}$$

The atomic velocities are denoted by $v_i(t)$ and Boltzmann's constant by k.

Normally, MD is performed at constant volume and constant total energy, yielding a microcanonical ensemble. In general, experimental conditions are constant temperature and pressure. Therefore, one would like to perform MD simulations under such conditions. This can be done by coupling the system to an external bath with constant temperature T_0 and a bath with constant pressure P_0 with adjustable time constants τ_T and τ_P of the couplings [30]. The coupling to the temperature bath is executed by adding the equation:

$$\frac{dT(t)}{d(t)} = \tau_T^{-1}[T_0 - T(t)] \tag{7}$$

The strength of the coupling to the temperature bath is determined by the temperature relaxation time τ_T in Eq. 7. For the coupling to the pressure bath a similar equation is used:

$$\frac{dP(t)}{dt} = \tau_p^{-1}[P_0 - P(t)] \tag{8}$$

where the strength of the coupling to the pressure bath is determined by the pressure relaxation time τ_P. Details about the algorithm for performing MD at constant T and P are provided in Ref. 30.

Computational procedure: Crystal simulation

Cyclosporin A crystallizes with two water molecules in space group $P4_1$. The dimensions of the unit cell are a = 1.3837 nm; b = 1.3837 nm; c = 4.1242 nm; $\beta = 90.0°$. It contains four cyclosporin A molecules with eight water molecules. The initial configuration for the simulation was obtained by applying the $P4_1$ symmetry transformations to the coordinates of cyclosporin A and the two water molecules. This unit cell coordinate set was used to build a computational box, which contains four unit cells. The dimensions of this box are 2a = 2.7674 nm, 2b = 2.7674 nm, c = 4.1242 nm; $\beta = 90.0°$. It contains 16 cyclosporin A molecules and 32 water molecules. So the crystal simulation contains 1536 atoms, involving 4608 degrees of freedom.

First the system was relaxed by performing 414 steps of conjugate gradients energy minimization (EM). Subsequently, the MD run was started by taking the initial velocities for the atoms from a Maxwellian distribution at 294 K. In order to avoid temperature drift, the system was weakly coupled to a heat bath of temperature $T_0 = 294$ K with a temperature relaxation time of $\tau_T = 0.1$ ps. During the first 2 ps, a strong coupling was applied ($\tau_T = 0.01$ ps). The MD simulation was performed at a constant pressure of 1 atm by coupling it to a pressure bath with a pressure relaxation time of $\tau_P = 0.5$ ps. The compressibility of the crystal was chosen as $\beta_T = 0.0001525$ kJ $mol^{-1}nm^{-3}$.

Periodic boundary conditions corresponding to the crystal translational symmetry were applied. The MD run covered a time span of 15 ps, which took about 165 central processing unit (CPU) hours on a VAX 11-750. The first 7 ps of the MD simulation were used to equilibrate the system. The time span from 7 to 15 ps was used for analysis and averaging. The crystal simulation will be denoted below by the symbol MDC.

Computational procedure: Solvent simulations

When modelling the structure of cyclosporin A in apolar solution, one isolated molecule is simulated, without applying periodic boundary conditions. Since the NMR experiments [18, 19] were performed in the apolar solvent $CDCl_3$, the omission of explicit solvent molecules is only a minor approximation. The NMR data were used in the simulation by applying restrained MD, i.e., the last term in Eq. 1 was taken into account. A set of 58 distance constraints was used. Out of these, 57 constraints were obtained from NOE measurements (see Fig. 2) [18]. The additional constraint corresponds with a hydrogen bond between the carbonyl oxygen of MeBmt and the

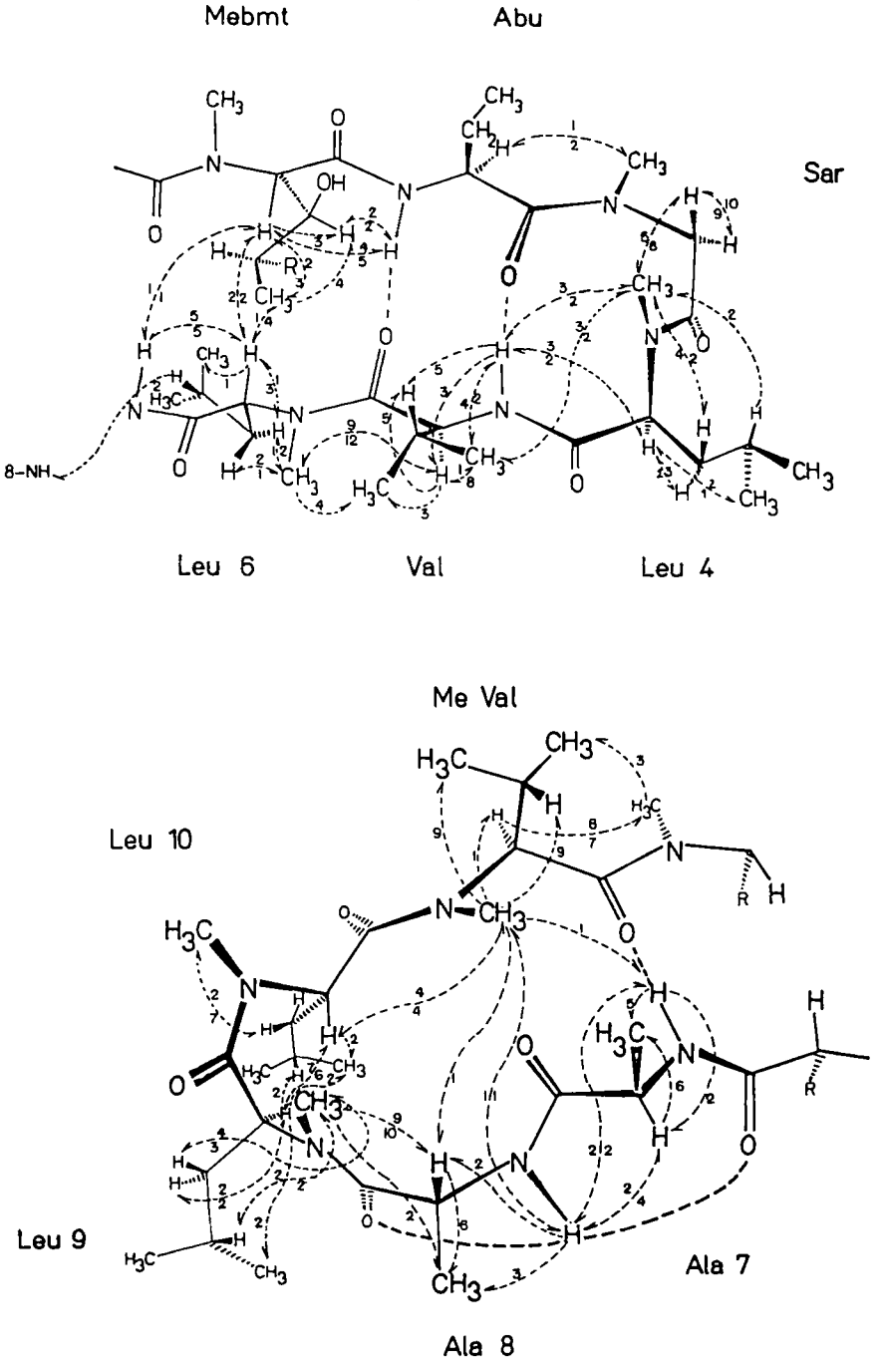

Fig. 2. Homonuclear proton-proton NOE effects of cyclosporin A in $CDCl_3$. All protons have been stereospecifically assigned. The numbers indicate the intensity of the NOE effect and are given in percent. One NOE (between 8 Ala-NH and 6 MeLeu-$C_\gamma H_3$: 6%) has been omitted from the list in Loosli et al., 1985, since it had been misassigned.

hydroxyl hydrogen of the MeBmt side chain. This hydrogen bond was detected by IR spectroscopy and its direction follows from the relatively small $C_\alpha H$-$C_\beta H$ coupling constant ($J = 5.7$ Hz) as discussed in Ref. 18. For this constraint, a distance r_{ij}^0 of 0.28 nm was used appropriate for this kind of H-bond [31,32].

The intensity of the NOE signals was translated into proton-proton distance constraints r_l^0 according to Table 1. For the translation of the NOEs into distance constraints, there is only one pair of protons, the geminal C_α-protons of sarcosine, that can be used for calibration purposes. This distance is about 0.18 nm and corresponds to a 9–10% NOE. We tried a rigid model approximation with r^{-6} distance dependence initially. However, this leads to too short distances for the smaller NOEs. Braun et al. [33] have shown that in flexible molecules the NOE has a less steep distance dependence. Taking this into account, we used a classification of NOE intensities and corresponding distance constraints r_l^0 as shown in Table 1. Although there is some arbitrariness in this procedure, the exact values of the distance constraints are not very critical, since in the restrained MD simulations the proton pairs are allowed to move within certain ranges in excess of the constraint distance ($\triangle r_l$) without large penalties in energy. Thus, in the initial runs on cyclosporin A, $\triangle r_l$ was 0.025 nm and in the final runs used for analysis $\triangle r_l$ was 0.05 nm. In the case of NOEs involving methyl groups, the constraints refer to a pseudo atom at the geometric mean of the three protons and a correction of 0.10 nm was added to the r_l^0 value [20].

We used the X-ray crystal structure as a starting structure for the first apolar solution simulation (MDS1). This structure was first minimized by restrained EM. Then the MD simulation was started in the same way as for the crystal simulation. The reference temperature we used was $T_0 = 300$ K, and a coupling to a heat bath of $T_0 = 300$ K with $\tau_T = 0.1$ ps was performed. The MD run covered a time span of 40 ps. During EM and the first 10 ps of the MD simulation, a force constant $K_{dc} = 4000$ kJ mol^{-1}nm^{-2} was used for the restraint potential in Eq. 2. This value allows r_{nm} to be about $\triangle r_l = 0.025$ nm larger than r_l^0 at a temperature of 300 K (contribution to the constraint energy is then $\frac{1}{2}$ kT). The value of 0.025 nm corresponds approximately to the experimental error in the distance constraints as determined from NOEs. From 10 to 40 ps a force constant of $K_{dc} = 1000$ kJ mol^{-1}nm^{-2} was applied which corresponds to a $\triangle r_l = 0.05$ nm and allows somewhat more flexibility to the molecule. We used the time span from 20 to 40 ps for analysis and averaging.

In addition the same procedure was repeated starting from the model built structure SMS [18]. For this MD calculation (MDS2), we used a force constant $K_{dc} = 1000$ kJ mol^{-1}nm^{-2} during the

TABLE 1
NOE INTENSITIES OBTAINED BY ONE-DIMENSIONAL ^{1}H NMR EXPERIMENTS AND CORRESPONDING PROTON-PROTON DISTANCE CONSTRAINTS[a]

NOE_{int} (%)	r_l^0(nm)
1.0 – 2.5	0.35
2.5 – 5.5	0.30
5.5 – 9.5	0.25
9.5 – 12.0	0.20

[a]The proton-proton distance constraints r_l^0 are defined in Eq. 2.

whole time span of 30 ps of the simulation. The time period between 10 to 30 ps was used for analysis and averaging. The simulation of 1 ps of a single cyclosporin A molecule took about 30 min CPU time on a VAX 11/750. The two vacuo simulations mimicking cyclosporin A in apolar solution are denoted below by the symbols MDS1 and MDS2.

RESULTS AND DISCUSSION

A. Comparison of X-ray and simulated (MDC) properties of CPA

The properties that are derived from the atomic trajectories in the MDC simulation of the crystalline state of CPA are compared here to the properties derived from the X-ray diffraction experiment [18]. This constitutes a test of the molecular model and force field that is applied in the simulation. The MDC simulation has been performed at a constant pressure of $P_0 = 1$ atm. This means that the volume of the computational box is a variable which adapts itself to the reference pressure P_0. After equilibration, the lengths of the three edges of the box are $L_a = 2.725$ nm, $L_b = 2.735$ nm and $L_c = 4.090$ nm. These values should be compared to the initial crystal values of $L_a = L_b = 2a = 2b = 2.7674$ nm and $L_c = c = 4.1242$ nm. So the density has changed from the experimental value of $\rho = 1.042$ g cm^{-3} to a value of $\rho_{MDC} = 1.080$ g cm^{-3}, a modest increase of 3.6%. Therefore, the atomic van der Waals radii are approximately correct.

Atomic positions and fluctuations

The average MD structure is obtained by averaging the atomic trajectories. This averaging also yields the atomic root mean square (rms) positional fluctuations:

$$\mathrm{Rms}_{\mathrm{pos.fluc}} = \Big[\sum_{\substack{i=1 \\ (x,y,z)}}^{N} < \overline{x_i^{MD} - < x_i^{MD} >}^2 > /N \Big]^{1/2} \tag{9}$$

where the summation i runs over a specified set of N atoms (e.g. C_α atoms or all atoms) and over the three Cartesian components. Averaging over time is denoted by $\overline{\ldots}$ and averaging over corresponding atoms in different asymmetric units is denoted by $< \ldots >$.

The average MD structure can be compared to the experimental X-ray structure in terms of the rms difference of the atomic positions:

$$\mathrm{Rms}_{\mathrm{pos.diff.}} = \Big[\sum_{\substack{i=1 \\ (x,y,z)}}^{N} (x_i^{exp} - < \overline{x_i^{MD}} >)^2 > /N \Big]^{1/2} \tag{10}$$

When comparing two structures, it is common practice to fit the two structures as good as possible to each other. One may perform a translational fit by superimposing the centers of mass of both structures (cm fit) and subsequently perform a least squares rotational fit (rot fit) around the shared center of mass. From the top part of Table 2, it can be seen that the agreement of the simulated with the X-ray structure is not really influenced by fitting. The backbone atom positions are reproduced within 0.03 nm, whereas the side-chain atoms may show much larger deviations.

The isotropic B-factors resulting from crystallographic refinement procedures may be converted to positional rms fluctuations using the formula

$$\mathrm{Rms}_{\mathrm{pos.fluc.}} = [3\ B_{\mathrm{iso}}/(8\pi^2)]^{1/2} \tag{11}$$

From the middle part of Table 2 it is observed that, in contrast to the positional averages, the rms fluctuations are influenced by translational and rotational fits. These fit procedures do remove the overall translational and/or rotational motion of the CPA molecules. The simulated fluctuations are of the correct size for the backbone atoms, but larger than those derived from the crystallographic B-factors for the side-chain atoms. This can be understood from the observation that crystallographic refinement procedures tend to underestimate the mobility of mobile atoms [34]. This is due to the harmonic approximation by which the electron density map is described. When two peaks of unequal intensity have to be described by one Gaussian curve, one will most likely be missed. From Fig. 3, it is observed that the atomic mobilities as a function of residue number for the simulation (dashed line) and experiment (solid line) are comparable. The difference in rms fluctuation is generally smaller than 0.02 nm, except for the side chains of 4 MeLeu and 11 MeVal.

TABLE 2
ATOMIC POSITIONAL DIFFERENCES[a] AND FLUCTUATIONS[a]

			Backbone				(Me)Leu side chains			
		All	N	C_α	C'	O	C_β	C_γ	$C_{\delta 1}$	$C_{\delta 2}$
Rms difference										
X-ray/$<\overline{\mathrm{MDC}}>$	no fit	0.060	0.023	0.028	0.029	0.052	0.038	0.081	0.162	0.129
	cm fit[b]	0.060	0.023	0.027	0.029	0.053	0.038	0.081	0.162	0.129
	cm/rot fit[c]	0.060	0.024	0.028	0.030	0.053	0.039	0.082	0.162	0.131
Rms fluctuation										
X-ray		0.051	0.044	0.044	0.044	0.050	0.053	0.061	0.70	0.067
$<\overline{\mathrm{MDC}}>$	no fit	0.084	0.069	0.070	0.069	0.080	0.079	0.086	0.124	0.120
	cm fit[b]	0.068	0.047	0.049	0.047	0.061	0.065	0.080	0.121	0.116
	cm/rot fit[c]	0.054	0.031	0.032	0.031	0.049	0.047	0.071	0.112	0.111
Ratio of smallest and largest fluctuation[d]										
X-ray		0.75	0.78	0.74	0.75	0.76	0.83	0.80	0.62	0.81
$<\overline{\mathrm{MDC}}>$	no fit[b]	0.50	0.51	0.51	0.50	0.48	0.58	0.54	0.47	0.50
	cm fit[c]	0.41	0.42	0.41	0.44	0.45	0.36	0.38	0.43	0.45
	cm/rot fit	0.44	0.54	0.53	0.57	0.40	0.41	0.33	0.35	0.40

[a]All differences and fluctuations are given in nm.

[b]The symbol 'cm fit' means that, before comparing two configurations, the second has been translated such that the centers of mass coincide.

[c]The symbol 'cm/rot fit' means that, in addition, a rotational least squares fit of the C_α atomic position has been performed.

[d]The ratio of smallest to longest principal axis of the anisotropic position fluctuation ellipsoids.

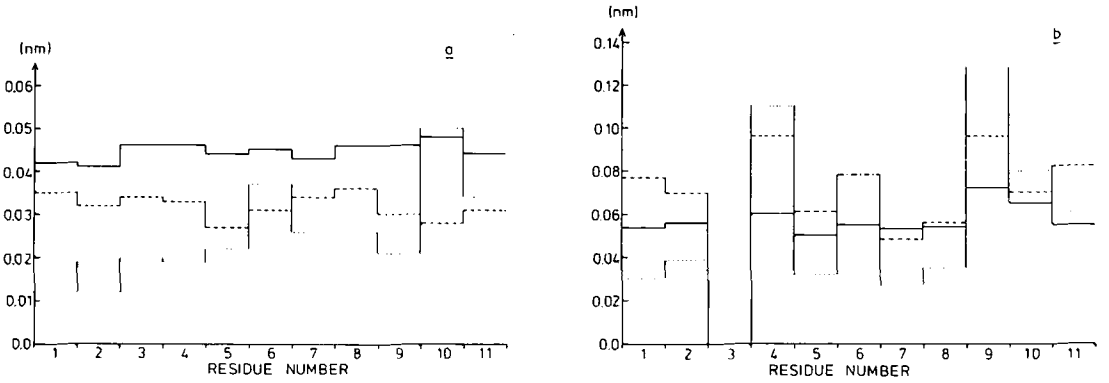

Fig. 3a. Rms positional fluctuations of the C_α atoms (nm). Solid line: as derived from crystallographic B-factors. Dashed line: from the $< \overline{MDC} >$ simulation. The rms positional difference between the X-ray structure and the $< \overline{MDC} >$ structure is given by the dotted line.
Fig. 3b. Like (a), but averaged over side-chain atoms.

We also note that the deviation of the MD positions from the X-ray ones (dotted line) is generally smaller than the experimental mobility (solid line) for the main chain atoms. Fig. 4 shows how close the $< \overline{MDC} >$ and X-ray structure are to each other. The side chains of 4 MeLeu and 9 MeLeu adopt a different orientation.

Dihedral angles

The backbone dihedral angles (Φ, Ψ, ω) are given in Table 3a for the X-ray structure and the $< \overline{MDC} >$ structure together with the rms fluctuation in brackets. For the majority of the dihedral angles the rms fluctuation is larger than the difference between X-ray and simulated values. Thus, the backbone conformation is well reproduced by the simulation.

Most of the side-chain dihedrals (Table 3b) are also within their rms fluctuation equal to those found in the X-ray structure. The fluctuations are increasing with the distance to the backbone atoms which is in accordance to the larger positional rms fluctuations found in the MDC simulation.

Hydrogen-bonding pattern

Hydrogen bonding determines quite strongly the secondary structure of peptides and proteins. We have used as a criterion for hydrogen bonding that the hydrogen-acceptor distance should be less than 0.25 nm and the D-H...A angle should be larger than 90°. The list of hydrogen bonds is given in Table 4. All hydrogen bonds found in the X-ray structure are reproduced by the MDC simulation. In addition, we find two hydrogen bonds forming γ-turns between 2 Abu-NH and 11 MeVal-O and 7 Ala-NH and 5 Val-O with a low occupancy. These two hydrogen bonds indicate a bending of the two-turn regions of cyclosporin A along an axis going through the C_α atoms of 1 MeBmt and 6 MeLeu.

In Table 5, the hydrogen bond pattern of the MDC simulation for the two crystalline water molecules is listed. These results indicate that the two water molecules are not strongly fixed in a specific orientation but are yet hydrogen bonded for at least half of the time during the simulation, whereas the X-ray geometry did not suggest any hydrogen bonding at all [18].

TABLE 3A

BACKBONE DIHEDRALS OF THE X-RAY STRUCTURE IN COMPARISON TO THE TIME AVERAGED DIHEDRALS OF THE CRYSTAL SIMULATION $<\overline{MDC}>$ AND THE SIMULATION USING RESTRAINTS $\overline{MDSI}$[a]

		X-ray[b]			$<\overline{MDC}>$[b]			$\overline{MDSI}$[b]		
		Φ	Ψ	ω	Φ	Ψ	ω	Φ	Ψ	ω
1	MeBmt	− 84	123	−175	− 91(9.4)	105(11.1)	−178(6.8)	−100(10.8)	95(11.0)	178(6.7)
2	Abu	−120	89	−178	−108(12.4)	100(10.3)	−180(9.0)	− 85(15.5)	97(8.9)	−159(8.6)
3	Sar	73	−129	173	59(10.0)	−117(9.7)	171(6.8)	57(9.6)	−116(9.9)	169(7.5)
4	MeLeu	− 99	21	180	−107(9.6)	31(16.0)	−179(6.2)	−113(9.6)	33(18.3)	176(6.8)
5	Val	−112	126	167	−119(14.3)	121(9.4)	163(8.0)	− 89(21.6)	120(9.6)	180(8.9)
6	MeLeu	− 90	99	−165	− 86(10.8)	108(12.1)	−174(6.7)	− 90(11.0)	96(11.1)	−179(6.1)
7	Ala	− 82	52	179	− 91(15.0)	61(21.7)	178(6.7)	− 90(14.2)	66(12.7)	178(6.9)
8	D-Ala	87	−124	−166	70(18.2)	−117(9.9)	−179(7.1)	80(17.2)	−128(10.9)	−177(7.4)
9	MeLeu	−119	99	− 5	−121(9.4)	121(11.0)	− 25(11.6)	−132(9.8)	113(13.0)	− 11(15.0)
10	MeLeu	−138	64	−167	−119(9.7)	94(10.1)	−171(13.1)	−121(11.4)	100(11.0)	−165(10.9)
11	MeVal	−102	125	173	−129(10.8)	116(11.5)	171(10.9)	−123(7.6)	104(11.5)	−172(11.9)

[a]The numbers in brackets denote the rms fluctuation obtained by averaging.

[b]All angles are given in degrees.

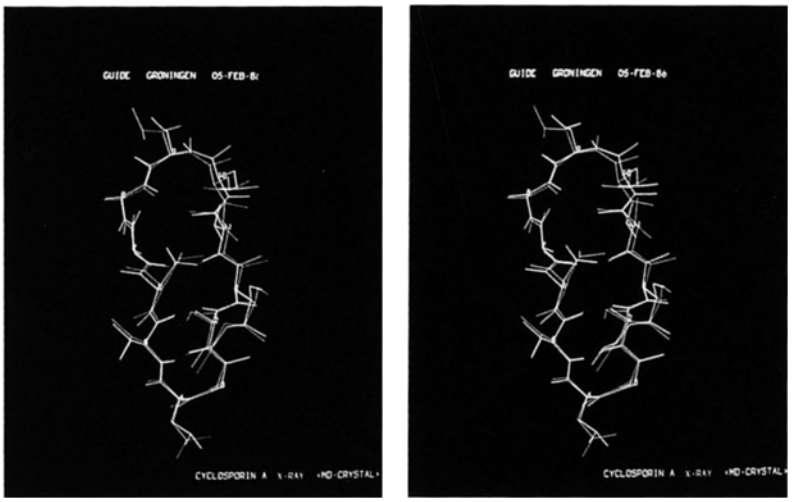

Fig. 4. Stereopairs of crystalline cyclosporin A. Blue: X-ray structure. Yellow: $< \overline{MDC} >$ structure. The polypeptide chain is shown with the residue sequence numbers running clockwise; the residue on top is 9 MeLeu, the one at the bottom is 4 MeLeu.

TABLE 3B
SIDECHAIN DIHEDRALS[a] OF THE X-RAY STRUCTURE AND THOSE OF THE SIMULATIONS

		X-ray	$<\overline{MDC}>$	$\overline{MDS1}$
1 MeBmt	χ_1	−166	−172(7.6)	− 67(9.7)
	χ_2	74	89(26.8)	163(15.2)
	χ_3	−179	−156(34.9)	−119(37.6)
	χ_4	−126	−155(30.5)	175(54.0)
	χ_5	−175	−179(7.4)[b]	180(8.1)
2 Abu	χ_1	−178	−150(40.0)	−125(50.1)
3 Sar	–	–	–	–
4 MeLeu	χ_1	− 51	− 95(22.7)	− 79(16.8)
	χ_2	− 54	−134(38.1)	− 80(22.7)
5 Val	χ_1	− 51	− 51(25.7)	− 63(10.3)
6 MeLeu	χ_1	−176	−163(23.7)	−173(14.0)
	χ_2	−177	−128(30.9)	−133(30.4)
7 Ala	–	–	–	–
8 D-Ala	–	–	–	–
9 MeLeu	χ_1	− 54	− 94(34.6)	− 72(14.8)
	χ_2	− 63	−100(32.8)	− 96(34.3)
10 MeLeu	χ_1	−163	−169(10.3)	−118(35.7)
	χ_2	−169	−152(26.5)	− 80(13.5)
11 MeVal	χ_1	− 53	− 62(28.6)	− 60(8.9)

[a]The dihedrals are given in degrees and the values in brackets denote the rms fluctuations obtained by averaging.
[b]Averaged over only 15 molecules, since one CPA molecule showed a complete 360° rotation of this dihedral angle.

TABLE 4
HYDROGEN BONDS[a] IN CYCLOSPORIN A LISTED FOR THE X-RAY STRUCTURE, THE $<\overline{MDC}>$ AND THE $\overline{MDS1}$ STRUCTURE

			X-ray				$<\overline{MDC}>$				$\overline{MDS1}$			
Donor		Acceptor	$d_{D...A}$	$d_{H...A}$	$\theta_{D-H...A}$	Occ.	$d_{D...A}$	$d_{H...A}$	$\theta_{D-H...A}$	Occ.	$d_{D...A}$	$d_{H...A}$	$\theta_{D-H...A}$	Occ.
1	MeBmt-OH	1MeBmt-O	–	–	–	–	–	–	–	–	0.282	0.211	128	84
1	MeBmt-OH	9MeLeu-O[b]	0.279	0.186	167.1	100	0.278	0.183	160.0	87	–	–	–	–
2	Abu-NH	5Val-O	0.284	0.184	171.2	100	0.295	0.203	154.5	96	0.310	0.221	150	61
2	Abu-NH	11MeVal-O	–	–	–	–	0.298	0.236	120.0	16	0.302	0.230	129	31
5	Val-NH	2Abu-O	0.302	0.207	153.5	100	0.289	0.197	153.9	96	0.300	0.207	157	88
7	Ala-NH	5Val-O	–	–	–	–	0.304	0.238	123.3	5	0.299	0.231	125	36
7	Ala-NH	11MeVal-O	0.298	0.196	162.1	100	0.296	0.202	158.0	97	0.306	0.212	159	89
8	Ala-NH	6MeLeu-O	0.290	0.198	151.1	100	0.301	0.218	139.8	62	0.301	0.217	141	69
8	Ala-NH	8Ala-O	–	–	–	–	–	–	–	–	0.267	0.240	95	2

[a]The criterion is: the donor-hydrogen acceptor angle $\theta_{D-H...A}$ must be larger than 90° and the donor-acceptor distance $d_{H...A}$ smaller than 0.25 nm. Distances d in nm, angles θ in degrees, occupancy (occ.) in %.

[b]Intermolecular hydrogen bond.

TABLE 5
CYCLOSPORIN-WATER HYDROGEN BONDS[a] WITH THE TWO WATER MOLECULES IN THE X-RAY STRUCTURE, OBTAINED FROM THE SIMULATION OF THE CRYSTAL STRUCTURE

Donor	Acceptor	$d_{D...A}$	$d_{H...A}$	$\theta_{D-H...A}$	Occ.
W1 OW-H	W2 OW	0.292	0.214	139.8	13
W2 OW-H	W1 OW	0.289	0.207	145.6	19
8 Ala N-H	W1 OW	0.304	0.216	150.0	26
1 MeBmt $O\gamma_1$-H	W2 OW	0.295	0.227	129.1	8
W1 OW-H	1 MeBmt O	0.294	0.210	146.5	36
W1 OW-H	6 MeLeu O	0.294	0.209	146.1	9
W2 OW-H	1 MeBmt $O\gamma_1$	0.303	0.224	142.0	11
W2 OW-H	7 Ala O	0.290	0.202	150.3	45
W2 OW-H	8 MeLeu O	0.295	0.222	132.0	13
W2 OW-H	10 MeLeu O	0.296	0.208	149.8	10

[a]The hydrogen bond criterion is the same as used in Table 4. Distances d in nm, angles θ in degrees, occupancy (occ.) in %. (W1, water molecule 1; W2, water molecule 2).

TABLE 6
REFINEMENT OF CYCLOSPORIN A

	Energy		NOE constraints	
Conformation	E_{pot}[a]	E_{dc}[b]	N_{viol}[c]	Σ_{viol}[d]
XRAY	631.24	40.8	7	0.62
EM1	62.5	25.0	8	0.47
MD 1 ps	15.1	7.4	6	0.22
MD 5 ps	− 23.6	6.0	8	0.20
MD 20 ps	− 22.1	0.5	4	0.03
MD 30 ps	− 37.9	2.7	6	0.16
MD 40 ps	− 19.6	7.9	4	0.22
$\overline{\text{MDS1}}$	-	0.3	4	0.04
SMS	764.6	0.01	1	0.01
EM2	− 45.7	0.2	5	0.03
MD 1 ps	36.4	9.1	7	0.26
MD 5 ps	− 17.3	0.5	5	0.07
MD 20 ps	− 26.3	8.0	9	0.29
MD 30 ps	− 42.5	3.8	7	0.18
$\overline{\text{MDS2}}$	-	0.9	5	0.08
$<\overline{\text{MDC}}>$	-	41.7	9	0.64

[a]E_{pot}: potential energy in kJ mol^{-1}.
[b]E_{dc}: potential energy associatated with NOE distance constraints (Eq. 2; a total number of 58 constraints was used in the EM and MD simulation.
[c]N_{viol}: total number of interproton distances larger than distance constraint r_l^0.
[d]Σ_{viol}: sum of interproton distances in excess of r_l^0 (nm).

B. Dynamic modelling of the solvent structure of CPA

When applying the dynamic modelling technique in order to obtain a solution structure, we started from the X-ray structure of CPA using the set of 58 distance constraints (Table 1, Fig. 2) obtained by NMR (see also Materials and Methods). The result of this MD simulation (MDS1) is compared to a MD simulation (MDS2) that was started from the model-built SMS structure [18] using the same set of distance constraints.

It can be seen from Table 6 that the structure in solution must be different from that in the crystal (X-ray) because for the latter the sum of all constraint violations is 0.62 nm. The SMS structure satisfies all constraints but it has a quite high potential energy of 764.6 kJ mol^{-1}, of which about half is due to Lennard-Jones interaction (365.2 kJ mol^{-1}). This indicates that there are close van der Waals contacts in the structure, which may be due to the fact that it was constructed by using model building techniques in connection with a minimization by a hardsphere potential [18]. The high potential energy of the X-ray structure is mostly due to a large bond energy term (359.9 kJ mol^{-1}), due to differences in ideal or standard bond lengths taken from the GROMOS force field and those used in the crystallographic refinement.

By restrained energy minimization (EM), the potential energy is brought down in both cases. Performing MD is a more efficient way to find low energy regions in configuration space, since the available kinetic energy allows the molecule to cross over barriers, which are of the order of kT ($\approx$2.5 kJ mol^{-1}; T = 300 K).

Starting from the crystal structure, the potential energy and the restraint energy decrease and after 5 ps fluctuates around equilibrium values. While in the second simulation starting from the SMS-model structure, the potential and restraint energy increase during the first pico seconds before they decrease and reach equilibrium. This indicates that a conformational change from one local minimum to another is occurring. Both refinement simulations lead to a structure that satisfies the set of distance constraints. The time-averaged structures show a total violation of the 58 constraints of 0.04 nm ($\overline{\text{MDS1}}$) and 0.08 ($\overline{\text{MDS2}}$).

TABLE 7
RMS DIFFERENCES OF ATOMIC POSITIONS BETWEEN SEVERAL STRUCTURES AS DEFINED IN EQ. 10

	C_α[a]	All atoms[a]
XRAY – $<\overline{\text{MDC}}>$	0.03	0.06
– $\overline{\text{MDS1}}$	0.09	0.18
– SMS	0.04	0.14
$<\overline{\text{MDC}}>$ – $\overline{\text{MDS1}}$	0.09	0.17
– SMS	0.06	0.16
$\overline{\text{MDS1}}$ – SMS	0.08	0.14
– $\overline{\text{MDS2}}$	0.02	0.05

[a]The rms differences are given in nm.

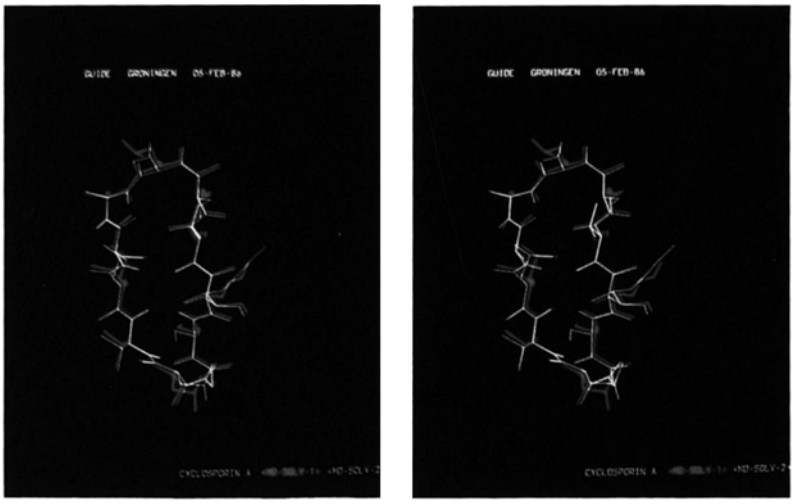

Fig. 5. Stereopairs of cyclosporin A in apolar solution. Red: MDS1 structure. Green: MDS2 structure.

Atomic positions

From Table 7 and Figs. 5 and 6, it can be seen how different the three solution structures of CPA (SMS, MDS1, MDS2) are. Both MD refinements, which start from configurations (X-ray, SMS) that differ by 0.04 nm (C_α atoms) and 0.14 nm (all atoms) from each other, converge to the same final structure (Fig. 5); the atomic positions in MDS1 and MDS2 differ only by 0.02 nm (C_α atoms) and 0.05 nm (all atoms), values which are smaller than the experimental atomic positional fluctuations. The SMS structure deviates much more from the MD refined ones (Fig. 6): 0.08 nm (C_α atoms) and 0.14 nm (all atoms). From the second and third line in Table 7, it can be concluded that the SMS structure is closer to the crystal structure (X-ray) than the MDS1 structure is. This observation reflects one of the advantages of dynamic modelling, in that it searches a larger part of configuration space than static modelling or EM procedures do.

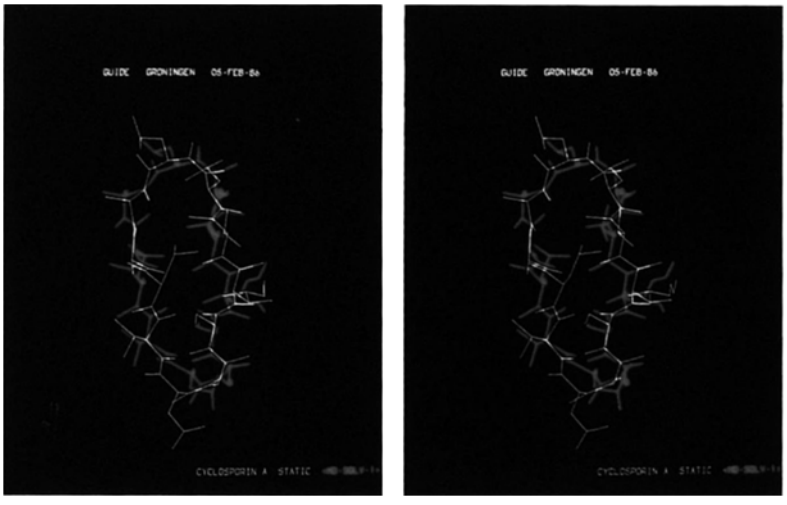

Fig. 6. Stereopairs of cyclosporin A in apolar solution. Red: MDS1 structure. Green: SMS structure.

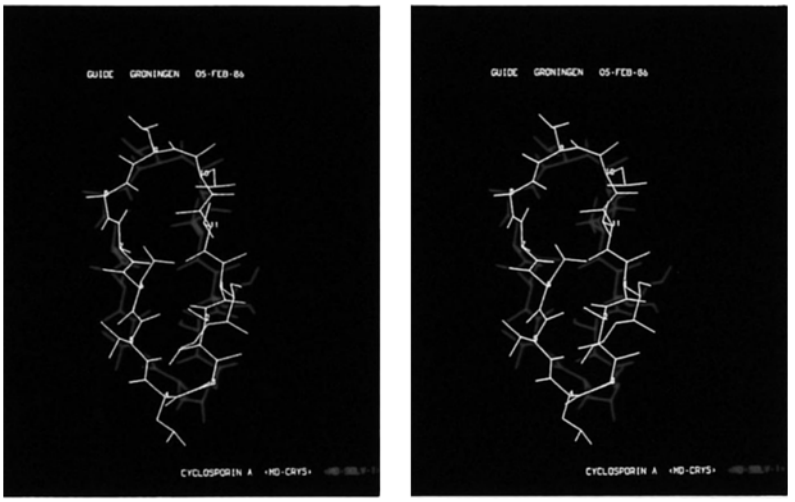

Fig. 7. Stereopairs of cyclosporin A in crystal and in solution. Yellow: $< \overline{MDC} >$ structure. Red: $\overline{MDS1}$ structure.

C. Comparison of structure and dynamics of CPA in solution and in the crystalline state

The differences between the structure and dynamics of CPA in the crystal and in solution are of interest for several reasons. The effect of a particular environment on the equilibrium conformation of a solute can be traced. From the practical point of view of understanding the immunosuppressive properties of CPA, knowledge of the structure and dynamics in solution may be helpful. Here we compare the solution structure ($\overline{MDS1}$) to the crystal structure ($< \overline{MDC} >$) has been obtained using the same force field. Since the simulated crystal structure ($< \overline{MDC} >$) is very close to the experimental one (X-ray), see Fig. 4 and Table 7, a separate comparison of the $\overline{MDS1}$ structure with the X-ray one would not add much information.

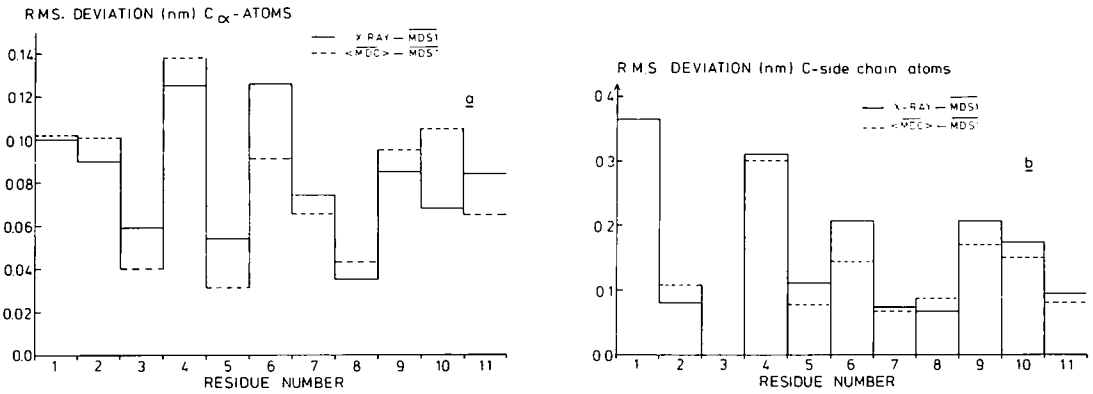

Fig. 8. Rms positional difference as a function of residue number between the crystal structure and the solution structure of cyclosporin A. Solid line: Difference between XRAY and $\overline{MDS1}$. Dashed line: Difference between $< \overline{MDC} >$ and $\overline{MDS1}$. (a) for the C_α atoms and (b) for the side-chain atoms.

Atomic positions

Fig. 7 shows the difference between the crystal structure and the solution structure of CPA. The backbone atoms show a rms difference of 0.09 nm (Table 7). When the side-chain atoms are also taken into account, the difference grows to 0.17 nm. Fig. 8 displays the difference as a function of residue number for both the C_α atoms and the side-chain atoms. The side chains of 1 MeBmt and 4 MeLeu show the largest differences ($\geqslant$ 0.3 nm).

Dihedral angles

The backbone dihedral angles for the $\overline{\text{MDS1}}$ structure are given in Table 3a together with the rms fluctuations within brackets. The largest differences between $\overline{\text{MDS1}}$ an $< \overline{\text{MDC}} >$ dihedrals occur for the residues 2 Abu ($\Delta\Phi = 23°$, $\Delta\omega = 21°$) and 5 Val ($\Delta\Phi = 30°$). CPA contains only four amide hydrogens, viz. in residues 2 Abu, 5 Val, 7 Ala and 8 Ala. For these residues, the allowed values for the Φ-dihedral can be deduced from NH-C_αH coupling constants [18] obtained by NMR, using a Karplus-type equation. The coupling constants and the corresponding Φ-values are: 2 Abu: $J_{exp} = 9.4$ Hz ($\Phi = 60°$ or $-100°$), 5 Val: $J_{exp} = 8.0$ Hz ($\Phi = 70°$, $50°$, $-89°$ or $-151°$), 7 Ala: $J_{exp} = 8.0$ Hz ($\Phi = 70°$, $50°$, $-89°$ or $-151°$), 8 D-Ala: $J_{exp} = 8.0$ Hz ($\Phi = -70°$, $-50°$, $89°$ or $151°$). The $\overline{\text{MDS1}}$ Φ-values (Table 3a) are consistent with the experimentally determined values.

Most of the side-chain dihedrals in the MDS1 structure are comparable to the X-ray and $< \text{MDC} >$ ones (see Table 3b), except for those in the 1 MeBmt and 10 MeLeu side chains. In solution the MeBmt side chain exhibits an extended conformation, whereas in the crystal it is folded over the backbone. The conformational change of the 10 MeLeu side chain may be related to the conformational change of the polypeptide backbone upon solvation of the CPA molecule.

Hydrogen bonding pattern

The hydrogen bonds found in the $\overline{\text{MDS1}}$ structure are given in Table 4. All hydrogen bonds that determine the two loop regions are the same as in the crystal structure. In addition we find the same two hydrogen bonds between 2 Abu-NH and 11 MeVal-O and 7 Ala-NH and 5 Val-O, which were also observed in the crystal simulation, but now with a higher occurrency. This indicates that the two loop regions are bending about an axis through the C_α atoms of 1 MeBmt and 6 MeLeu.

Based on heteronuclear Overhauser effect from the 8 Ala-NH to the neighboring carbonyl carbons [35], an additional hydrogen bond within the D-Ala 8 residue (8 Ala-NH ... 8 Ala-O) was proposed [18] which, however, could not be reproduced by the simulation; it occurs only for 2% of the time during the 20 ps which were used for averaging.

Fluctuations and flexibility

To obtain information about molecular flexibility of molecules in solution, one may determine the spin-lattice relaxation times T_1 of all C-atoms by ^{13}C NMR spectroscopy [18]. Under the assumption of a dipolar relaxation mechanism and isotropic molecular tumbling, the NT_1 values (N = number of attached protons at each C-atom) yield information about motions of the order of the Larmor frequencies. In flexible molecules, internal mobility adds to the overall tumbling rate of the molecule. Increasing NT_1 values indicate regional mobility in the molecule. We attempted to correlate the T_1 values with the atomic rms positional fluctuations of the MDS1-simulation according to Eq. 9. The result is given as a scatter plot in Fig. 9 [36–38]. The correlation for

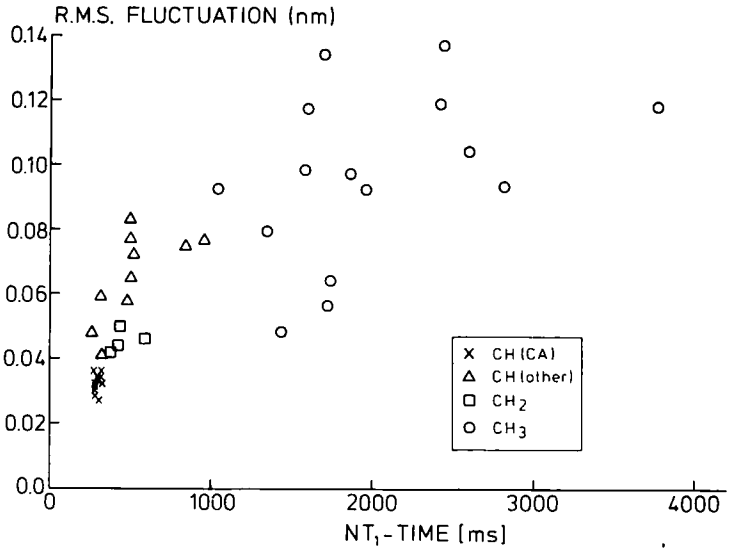

Fig. 9. Scatter plot of the simulated rms atomic positional fluctuation in solution (MDS1) against the experimental NT1 - C^{13} relaxation times of cyclosporin A in $CDCl_3$.

the C_α and C_β carbons is quite obvious, while for the outermost side chain atoms the correlation is less clear. Still, the pattern of increasing flexibility of the side chains fits with the experimental results. It is not very surprising that the correlation of the simulated side chain motion with the experimental T_1 values is not perfect. The simulation was performed in vacuo, without any solvent. In reality solvent molecules will dampen the motion of the side-chain atoms. Therefore it would be interesting to perform a MD simulation of CPA in water or an apolar solvent.

CONCLUSIONS

The molecular dynamics (MD) computer simulation studies that were described in this paper deal with three different, but related, aspects of modelling small polypeptides in the crystalline state and in solution.

1. In order to test the interatomic potential function or force field that is used in the MD simulations of polypeptides, a MD simulation of four unit cells of crystalline cyclosporin A (CPA), containing 16 CPA molecules and 32 water molecules was performed. The MD run covered 15 ps at constant temperature and pressure, and crystalline periodic boundary conditions were applied. The X-ray atomic positions were reproduced by the crystal simulation within 0.03 nm for the C_α atoms and within 0.06 nm for all atoms. These values are smaller than the experimentally observed atomic positional fluctuations. Also the hydrogen bond pattern is reproduced. These observations lead to the conclusion that the GROMOS force field that is used, yields an adequate representation of crystalline CPA.

2. On the basis of this force field and 58 atom-atom distance constraints that have been determined from NMR experiments, a solution structure of CPA has been derived by applying dynamic modelling techniques. MD simulations of an isolated CPA molecule have been performed in

which an extra term is added to the interatomic potential function. This term models the 58 distance constraints and so forces the molecule to adopt a conformation that satisfies the distance constraints. Starting from two different (0.14 nm) initial CPA structures, this distance restrained MD procedure converges to the same final solution structure of CPA. The advantage of this dynamic modelling technique over static model building on a graphics device is that it optimizes the energy of the molecule and the fit to the set of distance constraints simultaneously. Compared to energy minimization procedures, MD reaches a larger part of configuration space due to the presence of kinetic energy in the molecule which allows it to surmount barriers that are of the order of kT.

3. When the solution structure obtained is compared to the crystalline one, a few differences are observed. The overall difference in atomic positions is 0.09 nm for the C_α atoms and 0.17 nm for all atoms. The strongest deviation from the X-ray structure occurs in the β-pleated sheet (see Fig. 7), which is in agreement with X-ray structures of modified cyclosporin A molecules (H.P. Weber, personal communication), indicating that this region is much more flexible than one would expect. The two loop regions of the molecule are bending about an axis through the C_α atoms of 1 MeBmt and 6 MeLeu towards each other in solution. Furthermore, the side chains of 1 MeBmt and 10 MeLeu adopt different conformation in solution compared with the crystal.

Summarizing, we conclude that dynamic computer simulation techniques are very useful for refining model structures that are based on NMR data and for delineating conformational differences between molecules in solution and in the crystalline state.

ACKNOWLEDGEMENTS

The authors gratefully acknowledge Dr. H.-P. Weber and H.-R. Loosli (Sandoz AG, Basle, Switzerland) for providing us with the coordinates of the crystal and model built structures of cyclosporin A. Furthermore we want to thank Prof. P. Kollman (UCSF, San Francisco, USA) for stimulating discussions. One of the authors (J.L.) is supported by a grant of the DFG. We are grateful for the permission of Helvetica Chimica Acta to reproduce Figs. 1 and 2.

REFERENCES

1 Vida, J.A. and Gordon, M. (Eds.) Conformationally directed Drug Design, ACS Symposium Series 251, American Chemical Society, Washington, D.C., 1984.
2 Kessler, H., Angew. Chem. Int. Ed. Engl., 21 (1982) 512–523.
3 Matthews, B.W., Ann. Rev. Phys. Chem., 27 (1976) 493–523.
4 Kessler, H., Zimmerman, G., Förster, H., Engel, J., Oepen, G. and Sheldrick, W.S., Angew. Chem. Int. Ed. Engl., 20 (1981) 1053–1055.
5 Aue, W.P., Bartholdi, E. and Ernst, R.R., J. Chem. Phys., 64 (1976) 2229–2246.
6 Billeter, M., Braun, W. and Wüthrich, K., J. Mol. Biol., 155 (1982) 321–346.
7 Wagner, G. and Wüthrich, K., J. Mol. Biol., 155 (1982) 347–366.
8 Wider, G., Lee, K. and Wüthrich, K., J. Mol. Biol., 155 (1982) 367–388.
9 Arseniev, A.S., Wider, G., Joubert, F.J. and Wuthrich, K., J. Mol. Biol., 159 (1982) 323–351.
10 van Gunsteren, W.F., Kaptein, R. and Zuiderweg, E.R.P., In Olson, W.K. (Ed.) Proceedings of the NATO/CECAM Workshop on Nucleic Acid Conformation and Dynamics, Orsay, 1984, pp. 79–92.
11 Kaptein, R., Zuiderweg, E.R.P., Scheek, R.M., Boelens, R. and van Gunsteren W.F., J. Mol. Biol., 182 (1985) 179–182.

12 Clore, G.M., Gronenborn, A.M., Brünger, A.T. and Karplus, M., J. Mol. Biol., 186 (1985) 435–455.
13 Ruegger, A., Kuhn, M., Lichti, H., Loosli, H.R., Huguenin, R., Quiquirez, C. and von Wartburg, A., Helv. Chim. Acta, 59 (1976) 1075–1092.
14 Traber, R., Kuhn, M., Loosli, H.R., Lichti, H. and von Wartburg, A., Helv. Chim. Acta, 60 (1977) 1247–1255.
15 Traber, R., Kuhn, M., Lichti, H. and von Wartburg, A., Helv. Chim. Acta, 60 (1977) 1568–1578.
16 Wenger, R.M., Payne, T.G. and Schreier, M.H., Progress in Clinical Biochemistry and Medicine, Vol. 3, Springer Verlag, Berlin, 1986, pp. 157–191.
17 Wenger, R.M., Progress in Allergy, Vol. 38, Karger Medical and Scientific Publishers, Basel, 1986, pp. 46–64.
18 Loosli, H.R., Kessler, H., Oschkinat, H., Weber, H.P., Petcher, T.J. and Widmer, A., Helv. Chim. Acta, 60 (1985) 682–704.
19 Kessler, H., Loosli, H.R., Oschkinat, H., Helv. Chim. Acta, 60 (1985) 661–681.
20 van Gunsteren, W.F., Boelens, R., Kaptein, R., Scheek, R.M., Zuiderweg, E.R.P., In Hermans, J. (Ed.) Molecular Dynamics and Protein Structure, Polycrystal Book Service, P.O. Box 27, Western Springs, IL 60558, 1985, pp. 92–99.
21 Rose, G.D., Gierasch, L.M. and Smith, J.A., Adv. Protein Chem., 37 (1984) 1–109.
22 Chou, K.C., Pottle, M., Nemethy, G., Keda, Y. and Scheraga, H.A., J. Mol. Biol., 162 (1982) 89–112.
23 Hermans, J., Berendsen, H.J.C., van Gunsteren, W.F. and Postma, J.P.M., Biopolymers, 23 (1984) 1513–1518.
24 van Gunsteren W.F. and Karplus, M., Macromolecules, 15 (1982) 1528–1544.
25 Ryckaert, J.-P., Ciccotti, G. and Berendsen, H.J.C., J. Comput. Phys., 23 (1977) 327–341.
26 van Gunsteren, W.F. and Berendsen, H.J.C., Mol. Phys., 34 (1977) 1311–1327.
27 Berendsen, H.J.C., Postma, J.P.M., van Gunsteren, W.F. and Hermans, J., In Pullman, B. (Ed.) Intermolecular Forces, Reidel, 1981, pp. 331–342.
28 Wuthrich, K., Billeter, M. and Braun, W., J. Mol. Biol., 169 (1983) 949–961.
29 Hockney, R.W. and Eastwood, J.W., Computer Simulation Using Particles, McGraw-Hill, New York, 1981.
30 Berendsen, H.J.C., Postma, J.P.M., van Gunsteren, W.F., DiNola, A. and Haak, J.R., J. Chem. Phys., 81 (1984) 3684–3690.
31 Jolad, S.D., Hoffmann, J.J., Torrance, S.J., Wiedhopf, R.M., Cole, J.R., Arora, S.K., Bates, R.B., Gargiulo, R.L. and Krieg, G.R., J. Am. Chem. Soc., 99 (1977) 8040–8044.
32 Toniolo, C., CRC Crit. Rev. Biochem., 9 (1980) 2–44.
33 Braun, W., Bosch, C., Brown, L.R., Go, N. and Wuthrich, K., Biochim. Biophys. Acta, 66 (1981) 377–396.
34 Kuriyan, J., Petsko, G.A., Levy, R.M. and Karplus, M., J. Mol. Biol., 190 (1986) 227–254.
35 Khaled, M.A. and Watkins, C.L., J. Am. Chem. Soc., 105 (1983) 3363–3365.
36 Lipari, G. and Szabo, A., J. Am. Chem. Soc., 104 (1982) 4546–4559.
37 Lipari, G. and Szabo, A., J. Am. Chem. Soc., 104 (1982) 4559–4570.
38 Lipari, G., Szabo, A. and Levy, R.M., Nature, 300 (1982) 197–198.

ABBREVIATIONS

MeBmt: (4R)-4[(E)-2-butenyl]-4-methyl-L-Threonine.
MD: Molecular dynamics.
EM: Energy minimization.
MDC: Molecular dynamics simulation of the crystal.
MDS1: Restrained molecular dynamics simulation to obtain the structure in solution starting from the crystal structure.
MDS2: Like MDS1, but starting from the SMS structure.
SMS: Proposed structure in solution, obtained by model building.
XRAY: An X-ray structure.
CPA: Cyclosporin A.
NMR: Nuclear magnetic resonance spectroscopy.
NOE: Nuclear Overhauser enhancement.
$\overline{\text{MDS1}}$: Mean simulated structure obtained by averaging over the time period 20–40 ps of the MDS1 simulation.
$\overline{\text{MDS2}}$: Mean simulated structure obtained by averaging over the time period 10–30 ps of the MDS2 simulation.
$< \overline{\text{MDC}} >$: Mean simulated structure obtained by averaging over the time period 7–15 ps and over the 16 asymmetric units in the computational box of the MDC simulation.